



ELSEVIER

Cold Regions Science and Technology 34 (2002) 103–110

cold regions  
science  
and technology

www.elsevier.com/locate/coldregions

# Amount of unfrozen water in frozen porous media saturated with solution

Kunio Watanabe<sup>a,\*</sup>, Masaru Mizoguchi<sup>b</sup>

<sup>a</sup>*Department of Sustainable Resources, Faculty of Bioresources, Mie University, 1515 Kamihama, Tsu 514-8507, Japan*

<sup>b</sup>*Department of Biological and Environmental Engineering, The University of Tokyo, Tokyo 113-8657, Japan*

Received 6 February 2001; accepted 17 October 2001

## Abstract

In porous media, such as soil, some water do not freeze when cooled below 0 °C. The amount of unfrozen water is dependent on temperature and the characteristics of the porous media and solute in water. In this study, three types each of monosized glass powder, silty soil, and clay were saturated with various concentrations of NaCl, KCl, and MgCl<sub>2</sub> solutions and subjected to freezing temperatures. The relationship between the reduction in temperature and the amount of unfrozen water was measured using nuclear magnetic resonance (NMR) technique. The amount of unfrozen water decreased with the lowering of temperature. When a porous medium was saturated with a solution, the amount of unfrozen water increased with increasing solute concentration, in the order NaCl ≈ KCl < MgCl<sub>2</sub>. The resulting amount of unfrozen water was considered with respect to van der Waals and Coulombic interactions and the Gibbs–Thomson effect. The amount of unfrozen water in frozen glass powder and silty soil saturated with solution at concentrations lower than 0.1 mol l<sup>-1</sup> can be estimated when its Hamaker constant, specific surface area, distribution function, and initial solute concentration are given. © 2002 Elsevier Science B.V. All rights reserved.

*Keywords:* Unfrozen water; Solute concentration; Nuclear magnetic resonance methods; Porous media; Supercooling

## 1. Introduction

Even when cooled below 0 °C, some water in porous media, such as soil, remains unfrozen. The amount of unfrozen water in frozen porous media strongly depends on the temperature, and affects the strength and the hydraulic and thermal conductivity of the porous media. The hydraulic conductivity of soil drastically decreases as the temperature decreases (Burt and

Williams, 1976). The unfrozen water plays an important role in the freezing and thawing processes of porous media. As soil freezes, water migrates through subzero areas and sometimes forms ice lenses that cause severe frost heave (Horiguchi and Miller, 1980; Ishizaki, 1995; Watanabe and Mizoguchi, 2001).

The reason why water in porous media does not freeze at below bulk freezing temperature is attributed, in the main, to the melting point depression of the water, which is induced by adsorption forces and curvature at the particle surfaces. Since Faraday (1859) suggested that premelted (unfrozen) water might exist on the surface of ice, many studies concerned with surface melting of ice have been undertaken (Dash et al., 1995).

\* Corresponding author. Tel.: +81-59-231-9583; fax: +81-59-231-9571.

*E-mail address:* kunio@bio.mie-u.ac.jp (K. Watanabe).

It is now understood that a film of unfrozen water exists between the ice and the particle surface in frozen porous media, lowering the free energy of the system. The melting point of water is further depressed if it includes solutes, and this depends on the concentration of the solutes. These effects must be considered when considering the behavior and amount of unfrozen water in frozen porous media.

Many methods have been used to measure the amount of unfrozen water in frozen porous media, including isothermal calorimetry (Anderson and Tice, 1972), differential scanning calorimetry (Handa et al., 1992), nuclear magnetic resonance (NMR) methods (Tice et al., 1978), and time domain reflectometry (Spaans and Baker, 1995). Ishizaki et al. (1996) measured the amount of unfrozen water in frozen porous glass powder using an NMR technique and then evaluated the thickness of the layer of unfrozen water on the particle surface. Tice et al. (1984) introduced a technique for correcting the amount of unfrozen water resulting from high salt concentrations in partially frozen soil. The amount of unfrozen water is highly dependent on the physicochemical properties of the soil such as specific surface area, surface charge density, and the suite of exchangeable ions (e.g., Anderson and Tice, 1972). There are very few soils for which sufficient, high-quality data on unfrozen water exist. Changes in the amount of unfrozen water due to solute concentration are not well understood. Therefore, it is important to know how much unfrozen water exists in various frozen porous media. In this study, using a NMR technique, we measured the amount of unfrozen water in frozen glass powders, silty soil, and clay, saturated with different concentrations of solutions. The results are considered with respect to van der Waals and Coulombic interactions and the Gibbs–Thomson effect.

## 2. Materials and methods

### 2.1. Pulsed NMR methods

A proton of water bears a slight magnetic moment originating from its spin and acts as a magnet that tends to align along a fixed external magnetic field. The magnetic moment reorients when a pulse is applied to a sample set in a fixed magnetic field and

returns to its initial orientation when the pulse is eliminated. NMR measures the voltage induced by changes in the magnetic field. The voltage decay curve is called free-induction decay (FID). The peak FID value is proportional to the amounts of water and ice in the sample; the FID signal resulting from ice decreases more rapidly than the signal from liquid water. Therefore, we can determine the amount of liquid water (unfrozen water) in a sample from the FID value (Ishizaki et al., 1996).

### 2.2. Samples

The porous media that we used included three glass powders (GP9.7, GP5.3, and GP2.2), fujinomori soil (FJ), and bentonite (BN). Table 1 lists some characteristics of the porous media and Fig. 1 shows the pore size distribution of each medium. The mean diameter was estimated from electron micrographs. The pore size distribution, specific surface area, and specific nanopore volume were determined by nitrogen adsorption. Each glass powder consists of monodispersed particles and has frost susceptibility (Mutou et al., 1998; Watanabe and Mizoguchi, 2000). The particles are spherical with roughly the same diameter and their surfaces have nanopores with a uniform diameter (Fig. 1). Fujinomori soil is a silty soil with high frost susceptibility (Watanabe et al., 1997); bentonite is a swelling clay.

Distilled, deionized, and degassed water and NaCl, KCl, and  $MgCl_2$  of 99.9% purity were used. The saturated porous medium was prepared by placing the porous medium in a sealed chamber with the solution, evacuating the chamber, allowing a few days for solid–vapor equilibrium to be established, adding solution, and allowing the system to equilibrate for 1 day. The initial water contents and the solute concentrations of pore water are shown in Tables 1 and 2.

### 2.3. Test procedure

For NMR measurements, the prepared sample was compacted in a Teflon tube that was 25 mm in diameter and then sealed with a rubber stopper to prevent water evaporation. The tubes with samples were immersed in a temperature-controlled bath containing an ethylene glycol–water mixture as a coolant and allowed to reach a specified temperature. To measure

Table 1  
Characteristics of the porous media

Name	Glass powder			Fujinomori soil	Bentonite
	GP9.7	GP5.3	GP2.2	FJ	BN
Gravel (%)	0	0	0	0	0
Sand (%)	0	0	0	15	0
Silt (%)	97.3	45.9	12.6	61	0
Clay (%)	2.78	54.1	87.4	24	100
Mineral components	SiO <sub>2</sub> , Na <sub>2</sub> O (little), etc. (very little)	SiO <sub>2</sub> , Na <sub>2</sub> O (little), etc. (very little)	SiO <sub>2</sub> , Na <sub>2</sub> O (little), etc. (very little)	quartz, feldspar (little), kaolin, mica, montmorillonite, etc. (very little)	montmorillonite, etc.(very little)
Mean diameter of particle (μm)	9.7	5.3	2.2	–	–
Mean diameter of nanopore (nm)	3.3	3.3	3.1	–	–
Specific nanopore volume (cm <sup>3</sup> /g)	0.256	0.253	0.253	0.049	0.173
Specific surface area (m <sup>2</sup> /g)	150.5	146.4	128.6	29.9	80.9
Specific gravity of particle (g/cm <sup>3</sup> )	2.12	2.12	2.12	2.61	–
Dry powder density (g/cm <sup>3</sup> )	0.791	0.82	0.853	1.18	0.21
Initial water content (g <sub>water</sub> /g)	0.8	0.8	0.8	0.5	5

GP9.7, GP5.3, and GP2.2 are uniform-sized glass powders with mean diameters of 9.7, 5.3, and 2.2 μm, respectively. FJ and BN are fujinomori soil and bentonite, respectively.

the sample temperature, not the coolant temperature, a platinum resistance thermometer was inserted in a dry sample packed in an identical Teflon tube placed next to the sample tubes. After an equilibrium temperature was reached, the sample tube was removed from the bath, the peak FID value was measured, and then the tube was returned to the bath (Ishizaki et al., 1996).

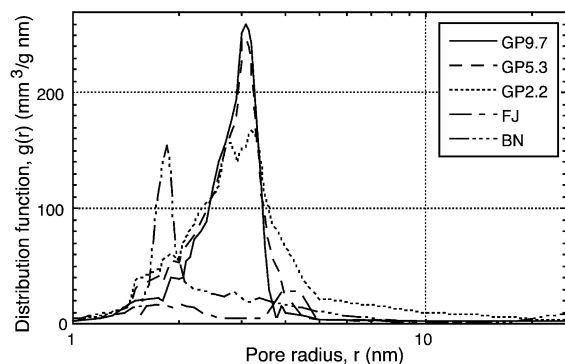


Fig. 1. Distribution curves of pores in the samples obtained by the nitrogen adsorption method.

A series of FID peak values was measured as the sample thawed from  $-50$  to  $+10$  °C, using a PRAXIS-2 pulsed NMR instrument. The applied magnetic field was 2.5 kG, the radio frequency was 10.7 MHz, and the pulse width was 12 μm. The amount of unfrozen water was then calculated from the FID value (Ishizaki et al., 1996). We assumed negligible melting and water migration in the sample during NMR measurement since the procedure was performed within 1 min, at an ambient temperature of 2 °C.

Table 2  
Initial solute concentration of pore water in FJ and BN

Solute	NaCl	KCl	MgCl <sub>2</sub>
Solute concentration (mol/l)	0	0	0
	0.0017	0.0013	0.0011
	0.0086	0.0067	0.0053
	0.017	0.013	0.011
	0.086	0.067	0.053
	0.17	0.13	0.11
	0.34	0.27	0.21
	0.51	0.4	0.32
	1.7	1.3	1.1

### 3. Results

The unfrozen water fraction,  $x$ , is calculated as the ratio of liquid water to total water in a porous medium; the ice fraction is  $1 - x$ .

Fig. 2 shows the unfrozen water fractions in the glass powders saturated with pure water (GP9.7, GP5.3, and GP2.2). In Fig. 2, there were two significant temperatures, near  $-1$  and  $-15$  °C, at which the slope of the unfrozen water fraction curve changed dramatically. As the temperature dropped below  $0$  °C, the amount of unfrozen water initially decreased steeply to half of the total amount of water, and subsequently decreased gradually. Even at  $-10$  °C, more than 30% of the water remained unfrozen. Below  $-15$  °C, the amount of unfrozen water decreased more slowly and reached about 5% of the initial amount at  $-40$  °C. As described in the following section, the melting point of water in nanopores with radii between 2 and 4 nm was depressed to  $-13$  and  $-6.5$  °C, respectively. Since the glass powders had many pores about 3 nm in radius (Fig. 1), they would contain large amounts of unfrozen water at between  $-1$  and  $-15$  °C. The glass powders GP9.7 and GP5.3 had similar unfrozen water fraction curves in spite of their different particle sizes. This may result from these powders having similar pore distributions (Fig. 1) and similar specific surface areas ( $\approx 150$  m<sup>2</sup> g<sup>-1</sup>). On the other hand, GP2.2, which had a different pore distribution (Fig. 1) and a smaller specific surface area (128.6 m<sup>2</sup> g<sup>-1</sup>), had slightly less unfrozen water

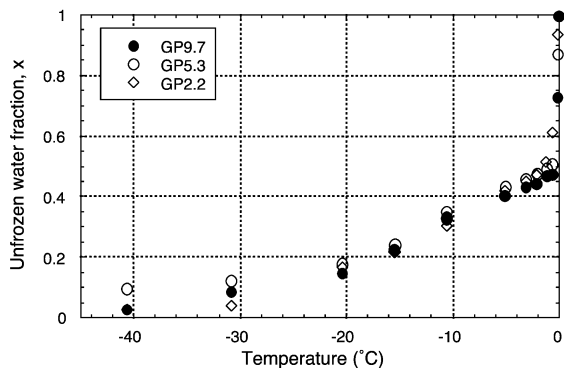


Fig. 2. Unfrozen water fraction in the glass powders. The initial water content of the sample is 80%, which corresponds to an unfrozen water fraction  $x = 1$ .

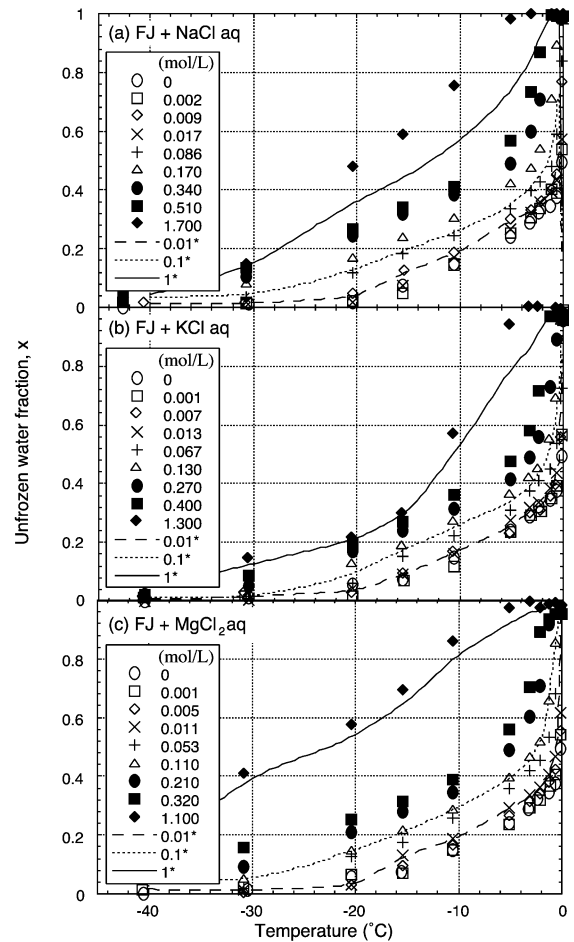


Fig. 3. Unfrozen water fraction in fujinomori soil (FJ). The soil was saturated with (a) NaCl, (b) KCl, and (c) MgCl<sub>2</sub> solutions. The initial water content was about 50%. In the figure, the Arabic numerals indicate the concentration of the solutes that the FJs are saturated with. The solid, dotted, and dashed lines indicate the concentration of 1, 0.1, and 0.01 mol l<sup>-1</sup> evaluated by interpolation.

at below  $-20$  °C and slightly more unfrozen water near  $0$  °C. These results suggest that the amount of unfrozen water in a frozen porous medium is strongly affected by the pore distribution and the specific surface area. In actual soil, there is a range of particle sizes with a consequent range in the distributions of pore space and surface area, which affect the amount of unfrozen water in the soil.

Figs. 3a–c and 4a–c show the respective unfrozen water fractions in fujinomori soil (FJ) and bentonite (BN) saturated with various concentrations of NaCl,

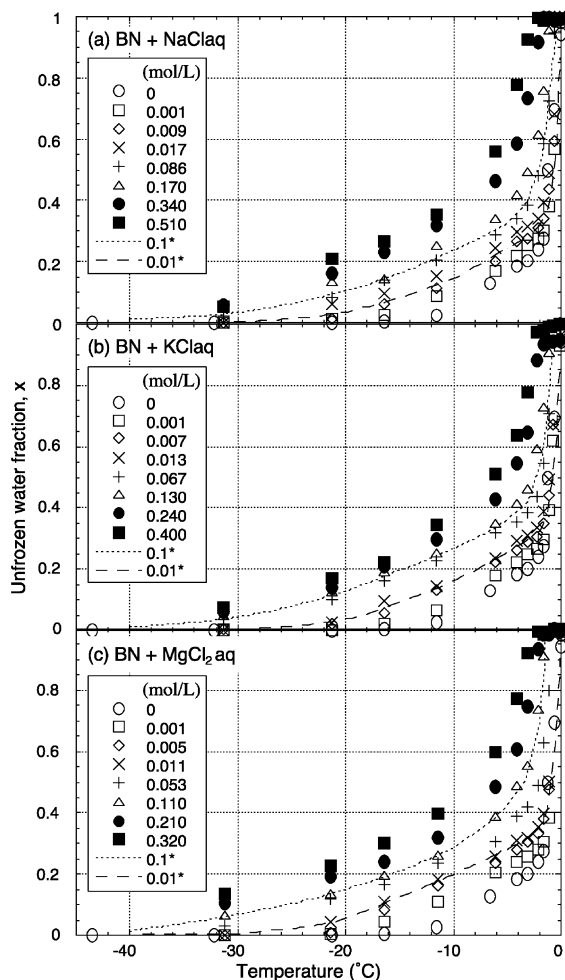


Fig. 4. Unfrozen water fraction in bentonite (BN). Bentonite was saturated with (a) NaCl, (b) KCl, and (c)  $MgCl_2$  solutions. The initial water content was about 500%. In the figure, the Arabic numerals indicate the concentration of the solutes that the BNs are saturated with. The dotted and dashed lines indicate the concentration of 0.1 and 0.01 mol  $l^{-1}$  evaluated by interpolation.

KCl, and  $MgCl_2$  solutions. In FJ and BN saturated with pure water, the amounts of unfrozen water decreased with temperature. No significant temperature, such as those shown in Fig. 2, was observed. In FJ and BN saturated with NaCl solution, the unfrozen water fractions maintained their initial value at temperatures a few degrees lower than 0 °C because of the melting point depression induced by the solute. Similar dependence of the unfrozen water fraction on the solute

concentration was also seen in FJ and BN saturated with KCl and  $MgCl_2$  solutions. The unfrozen water fraction curves for FJ and BN saturated with solutions at concentrations of 1, 0.1, and 0.01 mol  $l^{-1}$  were evaluated by interpolation (solid, dotted, and dashed lines in Figs. 3 and 4, respectively). Comparing the curves for fujinomori soils,  $FJ+MgCl_{2aq}$  had the most unfrozen water, and  $FJ+NaCl_{aq}$  had slightly more unfrozen water than  $FJ+KCl_{aq}$  (i.e.,  $FJ+MgCl_{2aq} > FJ+NaCl_{aq} \geq FJ+KCl_{aq}$ ). This tendency was stronger at higher solute concentrations. In bentonite, the amount of unfrozen water was in the following order:  $BN+MgCl_{2aq} > BN+KCl_{aq} \geq BN+NaCl_{aq}$ . The melting point of water is depressed according to the number of ions it contains. If the solutes have similar magnitudes of electrolytic dissociation, the  $MgCl_2$  solution contains more anions than other solutions, so that FJ and BN saturated with  $MgCl_2$  solution would contain more unfrozen water. The magnitude of electrolytic dissociation of the solutes, however, would vary with concentration and temperature. Some cations in solution would be exchanged on the clay surface. Differences in the electrolytic dissociation of the solute and the interaction between ions and clay surface may also affect the unfrozen water fraction curves.

## 4. Discussion

### 4.1. Amount of unfrozen water and the degree of supercooling

When ice contacts a foreign substrate below its bulk melting temperature, a thin film of unfrozen water exists on the surface of the substrate, which depends on intermolecular interactions (Dash et al., 1995). Consider a semi-infinite amount of ice separated by unfrozen water from a semi-infinite substrate. The van der Waals intermolecular energy per unit area between ice and the substrate is

$$F_{vdW}(d) = -\frac{A}{12\pi d^2}, \quad (1)$$

where  $d$  is the equilibrium thickness of the unfrozen water film and  $A$  is the Hamaker constant, which depends on the dielectric properties of all three materials in the layered system (Israelachvili, 1985).

The relationship between  $d$  and the degree of supercooling,  $T_m - T$ , is given by:

$$d^3 = -\frac{A}{6\pi\rho_s q} \left( \frac{T_m}{T_m - T} \right), \quad (2)$$

where  $T_m$  is the bulk melting temperature of water,  $\rho_s$  is the density of ice, and  $q$  is the latent heat of solidification per unit mass (Worster and Wettlaufer, 1999).

When any electrolyte is present in the film of unfrozen water between ice and a charged surface, the ions screen the Coulombic interaction with an efficiency that depends on the finite charge density  $q_s$  of the surface and the ion density of the electrolyte. For a monovalent electrolyte and a surface potential less than 25 mV, the excess interfacial free energy per unit area across an unfrozen water film of thickness  $d$  is approximated using the Debye–Hückel limit

$$F_{\text{DH}} \approx \frac{2q_s^2}{k\epsilon\epsilon_0} e^{-\kappa d}, \quad (3)$$

where  $\kappa^{-1} = (\epsilon\epsilon_0 kT/e^2 n_b)^{1/2}$ ,  $\epsilon$  is the dielectric constant of the film,  $\epsilon_0$  is the free space permittivity,  $k$  is the Boltzmann factor, and  $n_b$  is the bulk ion density (Wettlaufer, 1999). When the unfrozen water film is very thin, the approximation must be modified, but we will not deal with these complications here. Within the limits described, the total excess interfacial free energy of relevance to the unfrozen water film in the presence of electrolytes is the sum of  $F_{\text{vdW}}(d)$  and  $F_{\text{DH}}(d)$  (Eqs. (1) and (3)). Considering the situation in which the unfrozen water film includes a single species of monovalent nonvolatile electrolyte, there are a fixed number of electrolyte ions in the film, which maintain equilibrium with the interfacial charge. Wettlaufer (1999) presented the relationship between supercooling and the thickness of the unfrozen water film as

$$T_m - T = \frac{T_m}{\rho_l q} \left[ \frac{RT_m N_i}{d} - \frac{\Delta\gamma\sigma^2}{d^3} - \frac{\Delta\gamma c}{2} \sqrt{\frac{N_i}{d}} \right] \times \left( 1 + \frac{\sigma}{d} \right) \exp \left( -c \sqrt{\frac{N_i}{d}} (d - \sigma) \right), \quad (4)$$

where  $\rho_l$  is the molar density of the solvent,  $R$  is the gas constant,  $N_i$  is the number of moles per unit area of the electrolyte,  $\Delta\gamma$  is the difference in free energy between the dry and wet surfaces,  $\sigma$  is a short-range cutoff of

the order of molecular diameter, and  $c$  is a constant ( $7.237 \times 10^7 \text{ m}^{-1/2} \text{ mol}^{-1/2}$ ) when  $\kappa = c(N_i/d)^{1/2}$ .

In the case of water in a porous material, some water will not freeze at below its bulk freezing point as a result of the melting point depression due to curvature. The shift in freezing temperature,  $T_m - T$ , for a cylinder of ice of radius  $r$  is known as the Gibbs–Thomson effect:

$$T_m - T = \frac{T_m \gamma}{\rho_s q r}, \quad (5)$$

where  $\gamma$  is the ice–liquid water interfacial free energy.

#### 4.2. Calculating the amount of unfrozen water in frozen porous media

When a water-saturated porous medium is cooled below the bulk freezing temperature of water, as shown in Eqs. (2) and (4), unfrozen water films with a thickness of  $d(T)$  will exist on the particle surfaces. Assuming that water in the vicinity of the surface has the same density,  $\rho_w$ , as bulk water, therefore, a water-saturated porous medium with specific surface area,  $a$ , has an amount of unfrozen water per unit mass of  $U_s = ad(T)\rho_w$ . On the other hand, if the particles have nanopores on the surface, the water in the pores will not freeze until it has cooled to a temperature determined by the pore size. Here, we assume that all the pores on the surface are cylindrical and that the distribution of the internal radii of the cylinders follows the distribution function  $g(r)$ , as shown in Fig. 1. If the interfacial and size effects act independently, the water in a cylindrical pore with radius  $r(T)$  will remain unfrozen at a temperature,  $T$ , as described in Eq. (5). In this case, the porous medium has an amount of unfrozen water per unit mass of:

$$U_p = \int_0^{r(T)} g(r) dr. \quad (6)$$

Then, the total amount of unfrozen water per unit mass in a porous medium  $U_{\text{all}}$  can be calculated from the sum of these amounts of unfrozen water:

$$U_{\text{all}} = U_s + U_p = \rho_w \left( ad(T) + \int_{d(T)}^{r(T)} \left( \frac{r(T) - d(T)}{r(T)} \right)^2 g(r) dr \right), \quad (7)$$

where  $(r(T) - d(T))^2 / r(T)^2$  is a term that corrects the amount of unfrozen water on the surface in the pores.

The amount of unfrozen water in the glass powder with a diameter of  $9.7 \mu\text{m}$  was calculated (Fig. 5: GP9.7) using Eq. (7) and the following parameter values:  $a = 150.5 \text{ m}^2 \text{ g}^{-1}$ ,  $\gamma = 0.029 \text{ J m}^{-2}$ ,  $\rho_w = 998,000 \text{ g m}^{-3}$ ,  $\rho_s = 917,000 \text{ g m}^{-3}$ , and  $T_m = 273.15 \text{ K}$ . The distribution function  $g(r)$  was obtained from Fig. 1 and  $d(T)$  and  $r(T)$  were given by Eqs. (2) and (5), respectively. The Hamaker constant,  $A$ , for water on a solid surface generally takes a value from  $-10^{-19}$  to  $-10^{-20} \text{ J}$ . We tried various values of the Hamaker constant and found that the amount of unfrozen water in the glass powder was best predicted with  $A = -10^{-19.5}$  (Fig. 5). In the range  $T_m - T = 0 - 5 \text{ K}$ , most water in surface pores remained unfrozen and made up the majority of the total amount of unfrozen water. Pore water proceeded to freeze at  $T_m - T = 5 - 18 \text{ K}$ , causing the amount of unfrozen water to decrease. The strong peak in the distribution of pore size shown in Fig. 1 contributed to the sudden decrease in the amount of unfrozen water around  $T_m - T = 10 \text{ K}$  in Fig. 5. When  $T_m - T$  exceeded  $20 \text{ K}$ , the amount of unfrozen water virtually followed Eq. (2) and decreased in proportion to  $(T_m - T)^{-1/3}$ . With specific surface areas  $a = 146.5$  and  $128.6 \text{ m}^2 \text{ g}^{-1}$  and the respective  $g(r)$  shown in Fig. 1, the amount of unfrozen water in GP5.3 and GP2.2 was also calculated. The calculated values predict the amount of unfrozen water in water-saturated glass powders well (Fig. 5).

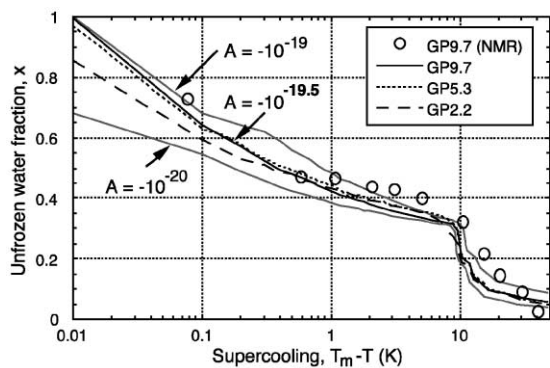


Fig. 5. Calculated amount of unfrozen water in glass powder. The calculated values for GP9.7 with three values of the Hamaker constant,  $A$ , are shown in the figure. (NMR) is the value measured using a NMR technique.

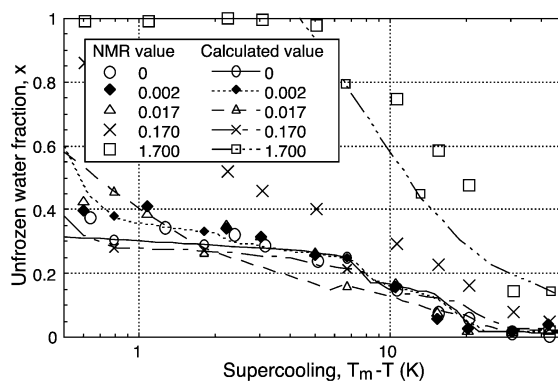


Fig. 6. Calculated amount of unfrozen water in fujinomori soil, compared with the value measured by the NMR technique.

With  $a = 24.5 \text{ m}^2 \text{ g}^{-1}$ ,  $R = 8.314 \text{ J mol}^{-1} \text{ K}^{-1}$ ,  $\sigma = 1.7 \times 10^{-10} \text{ m}$  (Azouni et al., 1997),  $\Delta\gamma = A / 12\pi\sigma^2 \text{ J m}^{-2}$  (Wettlaufer and Worster, 1995), and  $d(T)$  obtained from Eq. (4), the amount of unfrozen water in fujinomori soil saturated with various concentrations of NaCl solution was calculated in a similar way (Fig. 6). Soil is a very complex and heterogeneous system, and would not have a single value of the Hamaker constant. Using the value of the Hamaker constant for glass powders, the unfrozen water amount in fujinomori soil saturated with pure water was well predicted, so that we assume that the mean value of the Hamaker constant for fujinomori soil corresponds to the value used for the glass powders. With the lowering of temperature, the water in the soil started freezing at a supercooling degree,  $T_m - T$ , according to the solute concentration; subsequently, the amount of unfrozen water decreased. The calculated results were in good agreement with the experimental data at concentrations lower than  $0.1 \text{ mol l}^{-1}$ . The calculation tends to underestimate the amount of unfrozen water at higher concentrations, although the mechanism is still obscure. In addition, the calculation cannot deal with swelling clays, such as bentonite.

## 5. Conclusion

Using an NMR technique, the amounts of unfrozen water in frozen porous glass powders, fujinomori soil, and bentonite were measured. The amount of unfro-

zen water decreased with temperature. In the glass powders, a large amount of unfrozen water caused by nanopores was observed. When the porous medium was saturated with different solutions, the amount of unfrozen water increased with increasing solute concentration, in the order  $\text{NaCl} \approx \text{KCl} < \text{MgCl}_2$ .

The amounts of unfrozen water in glass powder saturated with pure water and in fujinomori clay saturated with NaCl solution were calculated while considering van der Waals and Coulombic interactions and the distribution of pores on the surface of the particles. It was found that the amount of unfrozen water in a porous medium at a given temperature could be estimated, if its Hamaker constant, specific surface area, distribution function, and initial solute concentration are known.

### Acknowledgements

The authors thank S. Akagawa and Y. Miyata for obtaining data on the sample characteristics.

### References

- Anderson, D.M., Tice, A.R., 1972. Predicting unfrozen water contents in frozen soils from surface area measurements. *Highw. Res. Rec.* 393, 12–18.
- Azouni, M.A., Casses, P., Sergiani, B., 1997. Capture or repulsion of treated nylon particles by an ice–water interface. *Colloids Surf., A* 122, 199–205.
- Burt, T.P., Williams, P.J., 1976. Hydraulic conductivity in frozen soils. *Earth Surf. Processes* 1, 349–360.
- Dash, J.G., Fu, H.-Y., Wettlaufer, J.S., 1995. The premelting of ice and its environmental consequences. *Rep. Prog. Phys.* 58, 115–167.
- Faraday, M., 1859. On regulation on the conservation of force. *Philos. Mag.* 17, 162–169.
- Handa, Y.P., Zakrzewski, M., Fairbridge, C., 1992. Effect of restricted geometries on the structure and thermodynamic properties of ice. *J. Phys. Chem.* 96, 8594–8599.
- Horiguchi, K., Miller, R.D., 1980. Experimental studies with frozen soil in an ice sandwich permeameter. *Cold Reg. Sci. Technol.* 3, 177–183.
- Ishizaki, T., 1995. Experimental study on unfrozen water migration in porous materials during freezing. *J. Nat. Disaster Sci.* 17, 65–74.
- Ishizaki, T., Maruyama, M., Furukawa, Y., Dash, J.G., 1996. Premelting of ice in porous silica glass. *J. Cryst. Growth* 162, 455–460.
- Israelachvili, J.N., 1985. *Intermolecular and Surface Forces*. Academic Press, London, UK.
- Mutou, Y., Watanabe, K., Ishizaki, T., Mizoguchi, M., 1998. Microscopic observation of ice lensing and frost heaves in glass beads. *Proc. 7th Int. Conf. Permafrost. Centre d'études nordiques université Laval, Quebec, Canada*, pp. 783–787.
- Spaans, E.J.A., Baker, J.M., 1995. Examining the use of TDR for measuring liquid water content in frozen soils. *Water Resour. Res.* 31, 2917–2925.
- Tice, A.R., Burrows, C.M., Anderson, D.M., 1978. Determination of unfrozen water in frozen soils by pulsed nuclear magnetic resonance. *Proc. 3rd Int. Conf. Permafrost. National Research Council of Canada, Canada*, pp. 149–155.
- Tice, A.R., Zhu, Y., Oliphant, J.L., 1984. The effects of soluble salts on the unfrozen water contents of the Lanzhov, P.R.C., Silt: CRREL Report, 84, 16–18.
- Watanabe, K., Mizoguchi, M., 2000. Ice configuration near a growing ice lens in a freezing porous media consisting of micro glass particles. *J. Cryst. Growth* 213, 135–140.
- Watanabe, K., Mizoguchi, M., 2001. Water and solute distribution near an ice lens in a glass–powder medium saturated with sodium chloride solution under unidirectional freezing. *Cryst. Growth Des.* 1, 207–211.
- Watanabe, K., Mizoguchi, M., Ishizaki, T., Fukuda, M., 1997. Experimental study on microstructure near freezing front during soil freezing. *Proc. Int. Symp. Ground Freezing. A.A. Balkema, Rotterdam, Netherlands*, pp. 187–192.
- Wettlaufer, J.S., 1999. Impurity effect in the premelting of ice. *Phys. Rev. Lett.* 82, 2516–2519.
- Wettlaufer, J.S., Worster, M.G., 1995. The dynamics of premelted films: frost heave in a capillary. *Phys. Rev. E* 51, 4679–4689.
- Worster, M.G., Wettlaufer, J.S., 1999. The fluid mechanics of premelted liquid films. In: Shyy, W., Narayanan, R. (Eds.), *Fluid Dynamics at Interfaces*. Cambridge Univ. Press, Cambridge, UK, pp. 339–351.